15 August 2000

Optics Communications 182 (2000) 281–288

OPTICS COMMUNICATIONS

www.elsevier.com/locate/optcom

Non-axisymmetric models for light scattering from a particle on or near a plane surface

A. Doicu [a,*], Yu. Eremin [b], T. Wriedt [a]

[a] Institut für Werkstofftechnik, Badgasteiner Straße 3, 28359 Bremen, Germany
[b] Department of Applied Mathematics and Computer Science, Moscow State University, Vorobyov Hills, 119899 Moscow, Russian Federation

Received 14 April 2000; received in revised form 19 June 2000; accepted 21 June 2000

Abstract

The communication is devoted to semi-analytical approaches for analyzing the scattering by a non-axisymmetric structure consisting of a nonspherical particle and a plane surface. On the basis of the discrete sources method and the *T*-matrix method, numerical schemes were developed and implemented in computer programs. Numerical results related to the influence of particle shape on the scattering characteristics are discussed. We will show that even for particles much smaller than the wavelength the scattering characteristics are still sensitive to the particle shape.

1. Introduction

The foregoing miniaturization of microchips come to be a real factor of a technical progress in semiconductor manufacturing. Being a first-step chain for the chip manufacturing, silicon wafers demand an extra care of their purity, which is determined by certain defects of real wafers: contaminating micro-particles, pits, subsurface bulks (crystal originated particles), scratches, etc. Therefore, the control of silicon wafer surface defects is of prime significance in semiconductor manufacturing. The purity monitoring is being carried out through optical surface scanners. The design of the surface scanner includes a laser source of light and collector's system to capture the intensity scattered by a micro-particle. Problems of surface scanner's operating include both false counts of non-existing contaminants detected, and missing counts of real defects not detected by the instrument. As the minimum line width of wafer structures continues to decrease, the importance of proper detection and characterization of scattering features grows. One response to this problem is the use of increasingly sophisticated models to predict light scatter signals using mathematical modeling and computer simulation analysis.

Several studies have addressed the scattering problem by spherical micro-particles [1–4]. In [5–8] the scattering by axisymmetric particles on a silicon substrate has been investigated in the framework of the discrete sources method and the *T*-matrix method. The analysis was restricted to an axisymmetric model by assuming that the particle symmetry axis coincides with the normal direction to the plane interface. Unfortunately, real contaminating particles are not

* Corresponding author. Tel.: +49-421-281-2318; fax: +49-421-218-5378; e-mail: doicu@iwt.uni-bremen.de

PII: S0030-4018(00)00830-0

axisymmetric. In this context the elaboration of mathematical models for such kind of applications appears to be of great interest in the design of surface scanners.

In the present communication, we extend our previous models [8] to a non-axisymmetric structure consisting in a nonspherical particle deposited on a plane surface. The aim of our analysis is to investigate the influence of the micro-particle shape on the scattering characteristics.

2. Discrete sources method

The geometry of the scattering problem is shown in Fig. 1. An arbitrarily shaped particle with a smooth boundary S and interior D_i is situated on a plane surface Σ. The upper half-space corresponding to the ambient medium is denoted by D_0, while the lower half-space corresponding to the substrate is denoted by D_1. Let us introduce a rectangular coordinate system $Oxyz$ by choosing the origin O at the tangent point between the particle and the substrate. The z-axis coincides with the normal direction to the plane surface Σ and is directed into the domain D_0. The wave number in the domain D_t, $t=0,1,i$, is denoted by $k_t = k\sqrt{\varepsilon_t \mu_t}$. The external excitation summing the contribution of the direct incident field and the reflected field will be denoted by $\boldsymbol{E}_{\mathrm{inc}}$, $\boldsymbol{H}_{\mathrm{inc}}$.

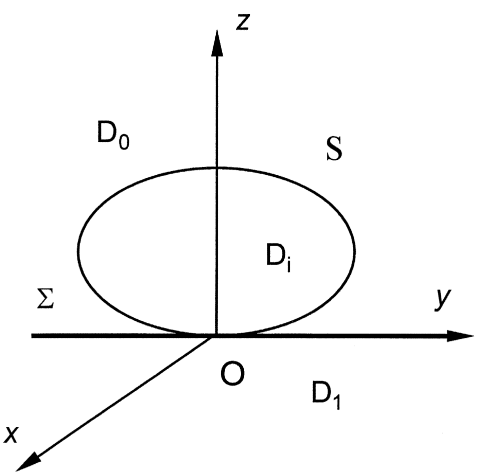

Fig. 1. Geometry of the scattering system.

The mathematical formulation of the scattering problem consists in the Maxwell equations

$$\nabla \times \boldsymbol{E}_t = jk\mu_t \boldsymbol{H}_t,$$
$$\nabla \times \boldsymbol{H}_t = -jk\varepsilon_t \boldsymbol{E}_t \quad \text{in} \quad D_t,\ t=0,1,i \tag{1}$$

the transmission conditions at the plane interface and the particle surface

$$\boldsymbol{e}_z \times (\boldsymbol{E}_1 - \boldsymbol{E}_0) = 0, \quad \boldsymbol{e}_z \times (\boldsymbol{H}_1 - \boldsymbol{H}_0) = 0 \ \text{on} \ \Sigma \tag{2}$$

and

$$\boldsymbol{n} \times (\boldsymbol{E}_i - \boldsymbol{E}_0) = 0, \quad \boldsymbol{n} \times (\boldsymbol{H}_i - \boldsymbol{H}_0) = 0 \ \text{on} \ S, \tag{3}$$

respectively, and the radiation (attenuation) condition at infinity. Here, $\boldsymbol{n}$ is the outward unit normal vector to S and $\boldsymbol{E}_t$, $\boldsymbol{H}_t$ stands for the total field in the domain D_t. Note that the total field in D_0 sums the contribution of the exciting and the scattered field, that is $\boldsymbol{E}_0 = \boldsymbol{E}_s + \boldsymbol{E}_{\mathrm{inc}}$ and $\boldsymbol{H}_0 = \boldsymbol{H}_s + \boldsymbol{H}_{\mathrm{inc}}$. If $\mathrm{Im}\ \varepsilon_t$, $\mu_t \geq 0$ and the particle surface is sufficiently smooth, then the above boundary-value problem is uniquely solvable.

We will construct an approximate solution to the scattering problem by representing the electromagnetic fields as a finite linear combination of fields of electric dipoles. The approximate solutions satisfy the Maxwell equations in the domains D_t, $t=0,1,i$, the radiation condition in the domains D_t, $t=0,1$, and the transmission condition at the plane interface. Essentially, the scattering problem simplifies to the approximation problem of the external excitation on the particle surface. The amplitudes of discrete sources will be determined from the transmission conditions (3).

For constructing the approximate solutions we consider the Green tensor for a stratified interface [9], that is

$$\overline{\overline{\boldsymbol{G}}}(\boldsymbol{r},\boldsymbol{r}_0) = \begin{bmatrix} G_{11} & 0 & 0 \\ 0 & G_{11} & 0 \\ \dfrac{\partial g}{\partial x} & \dfrac{\partial g}{\partial y} & G_{33} \end{bmatrix}, \tag{4}$$

where the tensor elements are given by

$$G_{11}(\boldsymbol{r},\boldsymbol{r}_0) = \exp(jk_0 R)/R + \int_0^\infty J_0(\lambda r)\,\nu_{11}(z,z_0,\lambda)\,\lambda\,\mathrm{d}\lambda, \quad (5)$$

$$G_{33}(\boldsymbol{r},\boldsymbol{r}_0) = \exp(jk_0 R)/R + \int_0^\infty J_0(\lambda r)\,\nu_{33}(z,z_0,\lambda)\,\lambda\,\mathrm{d}\lambda, \quad (6)$$

$$g(\boldsymbol{r},\boldsymbol{r}_0) = \int_0^\infty J_0(\lambda r)\,\nu_{31}(z,z_0,\lambda)\,\lambda\,\mathrm{d}\lambda. \quad (7)$$

Here, $r = \rho^2 + \rho_0^2 - 2\rho\rho_0\cos(\varphi - \varphi_0)$, (ρ, φ, z) are the cylindrical coordinates of the observation point $\boldsymbol{r}$, (ρ_0, φ_0, z_0) are the cylindrical coordinates of the source point $\boldsymbol{r}_0$, $R = [r^2 + (z - z_0)^2]^{1/2}$, and, for $z \geq 0$ and $z_0 > 0$, the spectral functions ν_{11}, ν_{33} and ν_{31} are given by

$$\nu_{11}(z,z_0,\lambda) = \frac{\mu_1 K_z^0 - \mu_0 K_z^1}{\mu_1 K_z^0 + \mu_0 K_z^1}\frac{1}{K_z^0} \times \exp\left[-K_z^0(z+z_0)\right], \quad (8)$$

$$\nu_{33}(z,z_0,\lambda) = \frac{\varepsilon_1 K_z^0 - \varepsilon_0 K_z^1}{\varepsilon_1 K_z^0 + \varepsilon_0 K_z^1}\frac{1}{K_z^0} \times \exp\left[-K_z^0(z+z_0)\right], \quad (9)$$

$$\nu_{31}(z,z_0,\lambda) = \frac{2(\mu_1\varepsilon_1 - \mu_0\varepsilon_0)}{(\mu_1 K_z^0 + \mu_0 K_z^1)(\varepsilon_1 K_z^0 + \varepsilon_0 K_z^1)} \times \exp\left[-K_z^0(z+z_0)\right], \quad (10)$$

where $K_z^t = (\lambda^2 - k_t^2)^{1/2}$, $t = 0, 1$.

We consider now an auxiliary smooth surface S^- enclosed in S. Let $\{\boldsymbol{r}_n\}_{n=1}^\infty$ be a dense sequence of points on S^- and let us choose in each point $\boldsymbol{r}_n$ three linear independent dipoles. The dipoles are oriented along the directions $\boldsymbol{e}_\rho$, $\boldsymbol{e}_\varphi$ and $\boldsymbol{e}_z$, where $(\boldsymbol{e}_\rho, \boldsymbol{e}_\varphi, \boldsymbol{e}_z)$ is a basis of a local cylindrical coordinate system. The vector potentials $\boldsymbol{A}_n^1$, $\boldsymbol{A}_n^2$ and $\boldsymbol{A}_n^3$ corresponding to the dipoles oriented along the directions $\boldsymbol{e}_\rho$, $\boldsymbol{e}_\varphi$ and $\boldsymbol{e}_z$, respectively, are given by

$$\boldsymbol{A}_n^1(\boldsymbol{r}) = G_{11}(\boldsymbol{r},\boldsymbol{r}_n)\cos(\varphi - \varphi_n)\,\boldsymbol{e}_\rho - G_{11}(\boldsymbol{r},\boldsymbol{r}_n)\sin(\varphi - \varphi_n)\,\boldsymbol{e}_\varphi + \left[\frac{\partial g}{\partial \rho}(\boldsymbol{r},\boldsymbol{r}_n)\cos(\varphi - \varphi_n) - \frac{1}{\rho}\frac{\partial g}{\partial \varphi}(\boldsymbol{r},\boldsymbol{r}_n)\sin(\varphi - \varphi_n)\right]\boldsymbol{e}_z, \quad (11)$$

$$\boldsymbol{A}_n^2(\boldsymbol{r}) = G_{11}(\boldsymbol{r},\boldsymbol{r}_n)\sin(\varphi - \varphi_n)\,\boldsymbol{e}_\rho + G_{11}(\boldsymbol{r},\boldsymbol{r}_n)\cos(\varphi - \varphi_n)\,\boldsymbol{e}_\varphi + \left[\frac{\partial g}{\partial \rho}(\boldsymbol{r},\boldsymbol{r}_n)\sin(\varphi - \varphi_n) + \frac{1}{\rho}\frac{\partial g}{\partial \varphi}(\boldsymbol{r},\boldsymbol{r}_n)\cos(\varphi - \varphi_n)\right]\boldsymbol{e}_z \quad (12)$$

and

$$\boldsymbol{A}_n^3(\boldsymbol{r}) = G_{33}(\boldsymbol{r},\boldsymbol{r}_n)\,\boldsymbol{e}_z. \quad (13)$$

Consequently, the approximate solutions in the domains D_t, $t = 0, 1$, read as

$$\boldsymbol{E}_t^{\mathscr{N}}(\boldsymbol{r}) = \sum_{n=1}^{N}\sum_{l=1}^{3} p_{nl}^t \nabla\times\nabla\times\boldsymbol{A}_n^l(\boldsymbol{r}),$$

$$\boldsymbol{H}_t^{\mathscr{N}}(\boldsymbol{r}) = -\frac{j}{k\mu_t}\nabla\times\boldsymbol{E}_t^{\mathscr{N}}(\boldsymbol{r}). \quad (14)$$

The approximate solution in the interior domain D_i will be expressed in terms of the vector potential

$$\hat{\boldsymbol{A}}_n^l(\boldsymbol{r}) = j_0(k_i|\boldsymbol{r} - \boldsymbol{r}_n|)\boldsymbol{e}_l, \quad (15)$$

as

$$\boldsymbol{E}_i^{\mathscr{N}}(\boldsymbol{r}) = \sum_{n=1}^{N}\sum_{l=1}^{3} p_{nl}^i \nabla\times\nabla\times\hat{\boldsymbol{A}}_n^l(\boldsymbol{r}),$$

$$\boldsymbol{H}_i^{\mathscr{N}}(\boldsymbol{r}) = -\frac{j}{k\mu_i}\nabla\times\boldsymbol{E}_i^{\mathscr{N}}(\boldsymbol{r}). \quad (16)$$

The completeness of the system of electric dipoles placed on the auxiliary surface S^- guarantee the convergence of the approximate solution to the exact solution in closed subsets of D_0 [9]. As mentioned before the above representations fulfilled the conditions of the scattering problem except the transmission condition at the particle surface. In fact this condition will be used to determine the amplitudes of discrete sources. Various schemes for amplitude determination are at our disposal. As it has been found stable results can be obtained by using pseudoinversion of an over-determined system of linear equations. After the amplitudes of discrete sources have been determined one can calculate the far-field pattern $\boldsymbol{E}_{s\infty}$ of the scattered field $\boldsymbol{E}_s$, i.e.

$$\boldsymbol{E}_s(\boldsymbol{r}) = \frac{\exp[jk_0 r]}{r}\boldsymbol{E}_{s\infty}(\theta,\varphi) + O\left(\frac{1}{r^2}\right) \text{ as } r\to\infty, \tag{17}$$

by using the asymptotic representation for the Sommerfeld integrals [5].

2.1. T-matrix method

For modeling the scattering problem in the framework of the *T*-matrix method we use the same notations as before but we choose the origin O inside the particle and at the distance z_0 above the plane interface. The external excitation will be expressed as a series of regular spherical vector wave functions (SVWF) $\boldsymbol{M}^1_{m'n'}(k_0\boldsymbol{r})$ and $\boldsymbol{N}^1_{m'n'}(k_0\boldsymbol{r})$, i.e.

$$\boldsymbol{E}_{\mathrm{inc}}(\boldsymbol{r}) = \sum_{n'=1}^{\infty}\sum_{m'=-n'}^{n'} D_{m'n'}\left[a_{m'n'}\boldsymbol{M}^1_{m'n'}(k_0\boldsymbol{r}) + b_{m'n'}\boldsymbol{N}^1_{m'n'}(k_0\boldsymbol{r})\right]. \tag{18}$$

Here, $D_{m'n'}$ is a normalization constant and is given by

$$D_{m'n'} = \frac{2n'+1}{4n'(n'+1)}\cdot\frac{(n'-|m'|)!}{(n'+|m'|)!}.$$

The expansion coefficients $a_{m'n'}$ and $b_{m'n'}$ are separated into two parts

$$a_{m'n'} = a^0_{m'n'} + a^R_{m'n'},$$
$$b_{m'n'} = b^0_{m'n'} + b^R_{m'n'}, \tag{19}$$

where $a^0_{m'n'}$ and $b^0_{m'n'}$ correspond to the direct incident field, while $a^R_{m'n'}$ and $b^R_{m'n'}$ correspond to the incident field reflected by the plane interface. The expressions for $a^R_{m'n'}$ and $b^R_{m'n'}$ contain the Fresnel reflection coefficients and a phase factor arising from the phase difference between the plane wave and its reflected wave in O.

The scattered field contains the contributions of the direct scattered field

$$\boldsymbol{E}^0_s(\boldsymbol{r}) = \sum_{n=1}^{\infty}\sum_{m=-n}^{n} D_{mn}\left[e_{mn}\boldsymbol{M}^3_{mn}(k_0\boldsymbol{r}) + f_{mn}\boldsymbol{N}^3_{mn}(k_0\boldsymbol{r})\right] \tag{20}$$

and the reflected or the interacting field

$$\boldsymbol{E}^R_s(\boldsymbol{r}) = \sum_{n=1}^{\infty}\sum_{m=-n}^{n} D_{mn}\left[e_{mn}\boldsymbol{M}^{3,R}_{mn}(k_0\boldsymbol{r}) + f_{mn}\boldsymbol{N}^{3,R}_{mn}(k_0\boldsymbol{r})\right], \tag{21}$$

where $\boldsymbol{M}^{3,R}_{mn}(k_0\boldsymbol{r})$ and $\boldsymbol{N}^{3,R}_{mn}(k_0\boldsymbol{r})$ denote the radiating SVWF reflected by the surface. The interacting field is a result of the scattered field reflecting off the surface and striking the particle. For $\boldsymbol{r}$ inside a sphere enclosed in the particle the reflected SVWF are given by:

$$\begin{pmatrix}\boldsymbol{M}^{3,R}_{mn}(k_0\boldsymbol{r})\\ \boldsymbol{N}^{3,R}_{mn}(k_0\boldsymbol{r})\end{pmatrix} = \sum_{n'=1}^{\infty}\sum_{m'=-n'}^{n'} D_{m'n'}\,\delta_{mm'} \times\left[\begin{pmatrix}\alpha^{mn}_{m'n'}\\ \gamma^{mn}_{m'n'}\end{pmatrix}\boldsymbol{M}^1_{m'n'}(k_0\boldsymbol{r}) + \begin{pmatrix}\beta^{mn}_{m'n'}\\ \delta^{mn}_{m'n'}\end{pmatrix}\boldsymbol{N}^1_{m'n'}(k_0\boldsymbol{r})\right], \tag{22}$$

where $\delta_{mm'}$ stands for the Kronecker symbol. Substituting (22) into (21) we obtain a representation of the interacting field in terms of regular SVWF, i.e.

$$\boldsymbol{E}^R_s(\boldsymbol{r}) = \sum_{n'=1}^{\infty}\sum_{m'=-n'}^{n'} D_{m'n'}\left[e^R_{m'n'}\boldsymbol{M}^1_{m'n'}(k_0\boldsymbol{r}) + f^R_{m'n'}\boldsymbol{N}^1_{m'n'}(k_0\boldsymbol{r})\right], \tag{23}$$

where

$$\begin{pmatrix}e^R_{m'n'}\\ f^R_{m'n'}\end{pmatrix} = \sum_{n=1}^{\infty}\sum_{m=-n}^{n} D_{mn}\,\delta_{mm'}\left[\begin{pmatrix}\alpha^{mn}_{m'n'}\\ \gamma^{mn}_{m'n'}\end{pmatrix}e_{mn} + \begin{pmatrix}\beta^{mn}_{m'n'}\\ \delta^{mn}_{m'n'}\end{pmatrix}f_{mn}\right]. \tag{24}$$

In the *T*-matrix method the scattered field coefficients are related to the expansion coefficients of the fields striking the particle by the transition matrix. Truncating the expansions given in (18), (20) and (23) we obtain the following matrix equation for the scattering problem:

$$\begin{bmatrix}e_{mn}\\ f_{mn}\end{bmatrix} = [T^{mn}_{m'n'}]\cdot\left(\begin{bmatrix}a_{m'n'}\\ b_{m'n'}\end{bmatrix} + \begin{bmatrix}e^R_{m'n'}\\ f^R_{m'n'}\end{bmatrix}\right). \tag{25}$$

The explicit form of the transition matrix $[T_{m'n'}^{mn}]$ can be found in [10,11]. Relying on (24) it is readily seen that we may express the relation between the expansion coefficients of the interacting and the direct scattered fields in matrix form as

$$\begin{bmatrix} e_{m'n'}^{R} \\ f_{m'n'}^{R} \end{bmatrix} = [\, A_{m'n'}^{mn} \,] \cdot \begin{bmatrix} e_{mn} \\ f_{mn} \end{bmatrix}. \tag{26}$$

Here, $[\, A_{m'n'}^{mn}]$ stands for the so called reflection matrix. The scattered field coefficients e_{mn} and f_{mn} are obtained by combining matrix Eqs. (25) and (26). Explicit expressions for the incident field coefficients $a_{m'n'}$ and $b_{m'n'}$, and the elements of the reflection matrix are given in [7].

The main steps of the T-matrix approach are summarized as follows: calculation of the transition matrix which relates the expansion coefficients of the fields striking the particle to the scattered field coefficients; calculation of the reflection matrix characterizing the reflection of SVWF by the surface; computation of an approximate solution of the governing matrix equation, and extrapolation of the scattered field to the far field.

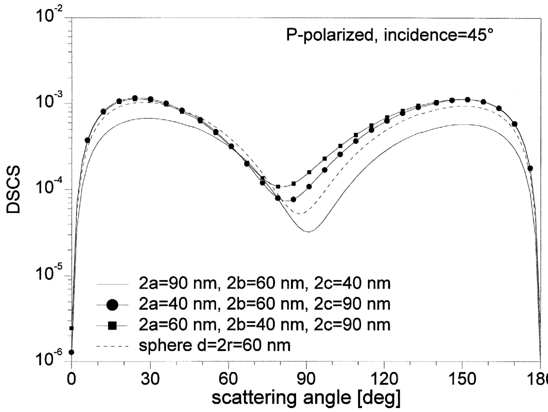

Fig. 3. Differential scattering cross-section for SiO-ellipsoids.

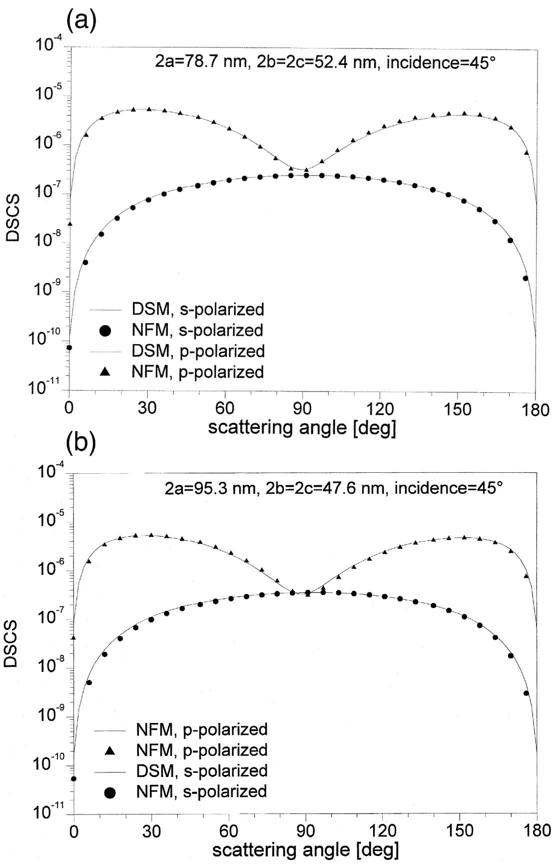

Fig. 2. Differential scattering cross-section (DSCS) for SiO-spheroids: (a) $2a = 78.7$ nm, $2b = 52.4$ nm and (b) $2a = 95.3$ nm, $2b = 47.6$ nm.

We want to point out that in the case of non-axisymmetric particles the scattering problem does not decouple over the azimuthal modes. Consequently, the amount of storage required for solving the scattering problem increases considerably.

3. Numerical simulations

In this section we investigate from a computational point of view the influence of particle shape on the response of a surface scanner. Usually, the diameter of the contaminating particles is much smaller than the diameter of a laser beam. In this context the assumption that the exciting field is a polarized plane wave seems to be realistic. In addition, since the diameter of the particle is smaller than the exciting wavelength, we restrict our analysis to the scattering by Rayleigh particles. Note, that the common wavelength used in particle contamination characterization is $\lambda = 488$ nm.

The first goal of our numerical simulations is to compare our computer codes based on the discrete sources method and the T-matrix method. We compute the differential scattering cross-section (DSCS)

Table 1
Spheroid sizes

a/b	$2a$ (nm)	$2b$ (nm)
1.0	60.0	60.0
1.5	78.7	52.4
2.0	95.3	47.6
2.5	110.3	44.2
3.0	124.4	41.6
3.5	138.0	39.4
4.0	151.7	37.7

for prolate spheroids with the axis of symmetry parallel to the plane surface. In this case the scattering structure is not axisymmetric and general models should be employed. The scatterers are SiO-particles with a refractive index of 1.67 deposited on a silicon substrate with a refractive index of $4.37 + 0.08j$. Assuming the incident field to have unit amplitude we evaluate the DSCS in the azimuthal plane $\varphi = 0$, which corresponds to the plane of incidence. The wavelength of the incident radiation is chosen to be $\lambda = 488$ nm, and the angle of incidence is $\beta = 45°$. The results plotted in Fig. 2 correspond to prolate spheroids with: (a) $2a = 78.7$ nm, $2b = 52.4$ nm and (b) $2a = 95.3$ nm, $2b = 47.6$ nm. In both cases the spheroids have the same equivolumetric diameter $d = 2r = 60$ nm. The agreement between the scattering curves certifies the validity of our methods. We want to point out that the numerical instabilities associated with the T-matrix computations for prolate spheroids having a horizontal axis of symmetry and touching the interface, are unnoticeable due to the small sizes of the scatterers.

In the next example we use the T-matrix method to analyze the influence of the particle shape on the

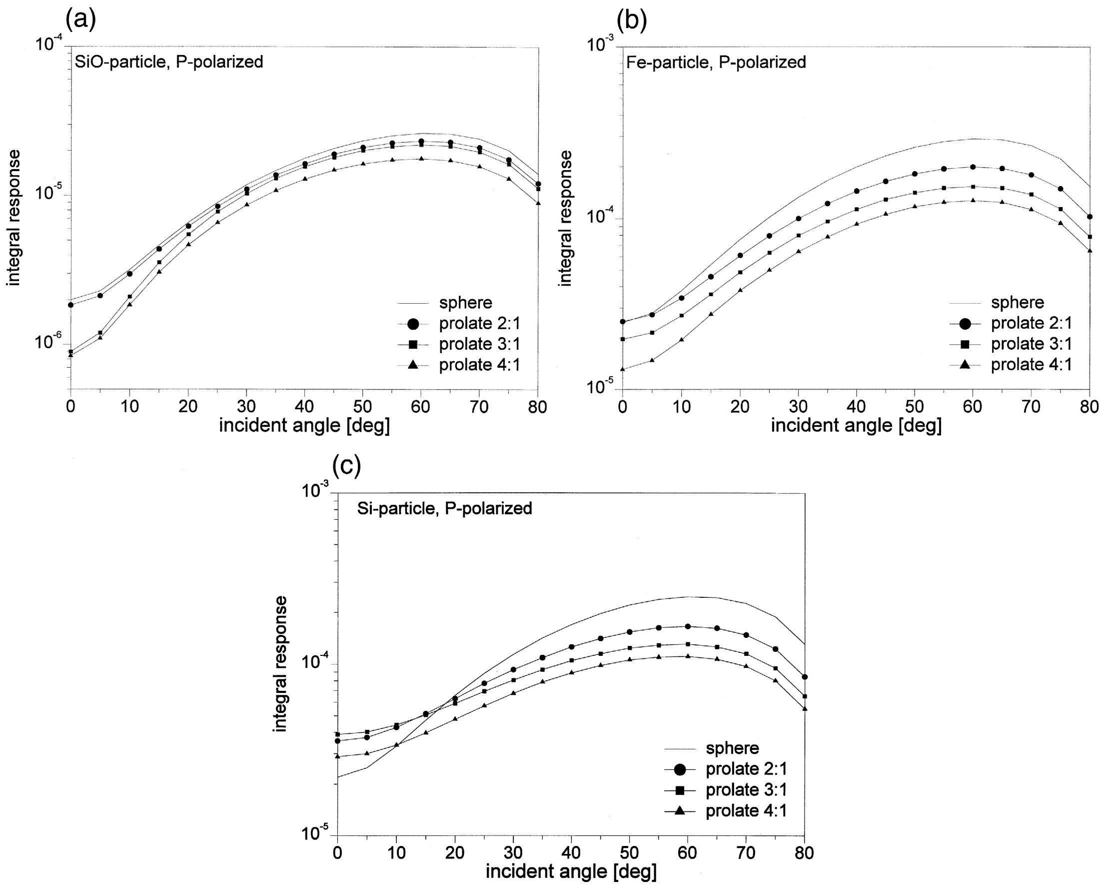

Fig. 4. Integral response versus the incident angle for: (a) SiO-spheroids, (b) Fe-spheroids and (c) Si-spheroids.

scattering characteristics. In Fig. 3 we compute the differential scattering cross-section for SiO-ellipsoids with: $2a = 40$ nm, $2b = 60$ nm, $c = 90$ nm; $2a = 60$ nm, $2b = 40$ nm, $2c = 90$ nm and $2a = 90$ nm, $2b = 60$ nm, $2c = 40$ nm. As before, all the spheroids have the same equivolumetric radius $d = 2r = 60$ nm. It is readily seen that modifications of the particle shape generate modifications of the scattering characteristics.

Next we will investigate the influence of the particle shape on the integrated scattering characteristics. We expect these influence to be more reduced for these quantities. For this purpose we compute the integral response

$$R^{P,S} = \int_{\Omega} |\boldsymbol{E}_{s\infty}^{P,S}|^2 \,\mathrm{d}\omega, \tag{27}$$

where Ω is the unit sphere, and the far-field patterns $\mathbf{E}_{s\infty}^{P}$ and $\mathbf{E}_{s\infty}^{S}$ correspond the P- and S-polarization of the incident plane wave. The integral response is computed by using the discrete sources method. The scatterers are prolate spheroids with the major axis parallel to the plane surface. The sizes of spheroids are given in Table 1.

Since contaminating micro-particles may be of different materials we will examine scattering by SiO-particles, Fe-particles with a refractive index of $1.35 + 1.97j$ and Si-particles with a refractive index of $4.37 + 0.08j$. Fig. 4a shows the dependency of the integral response of SiO-particles on the incident angle. As before the incident plane is the Oxz-plane. Similar results are plotted in Fig. 4b and c for Fe-particles and Si-particles, respectively. The plotted data show that the differences between the integral responses of a sphere and a spheroid are relatively small for SiO-particles and increase for Fe- and Si-particles. This behaviour is also illustrated in Fig. 5. Here, we plot the dependence of the integral response on the aspect ratio of the spheroids. We want to point out that the analysis has been performed for particles with an equivolumetric diameter smaller than 1/8 of the exciting wavelength. From the above analysis we may conclude that for small particles with the same equivolumetric diameter the integrated scattering characteristic is still sensitive to the particle shape. The deviations of the scattering characteristics with respect to that of a spherical particle are more pronounced when the refractive index increases.

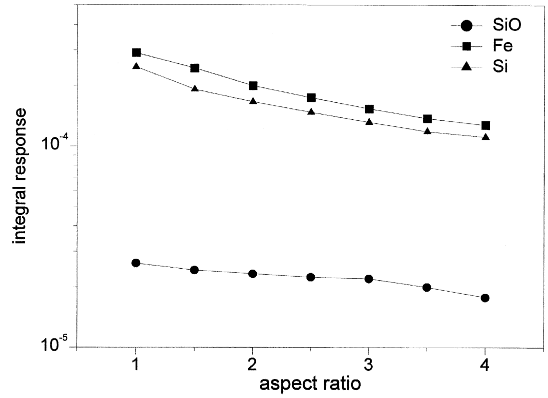

Fig. 5. Integral response versus the aspect ratio of prolate spheroids.

4. Conclusion

The discrete sources method and the T-matrix method have been extended to analyze the scattering characteristics of a non-axisymmetric structure consisting in a non-spherical particle and a plane surface. The computer results have shown a visible dependence of the scattering characteristics on the particle shape especially for particles with high refractive index. These results needs to be accounted in the design of surface scanners.

Acknowledgements

This research was supported by DAAD (ref. 325, N A/99/09581).

References

[1] P.A. Bobbert, J. Vlieger, Light scattering by a sphere on a substrate, Physica 137A (1986) 209–242.
[2] G. Videen, Light scattering from a sphere on or near a surface, J. Opt. Soc. Am. A 8 (1991) 483–489.
[3] G. Videen, Scattering from a small sphere near a surface, J. Opt. Soc. Am. A 10 (1993) 118–126.
[4] B.K. Johnson, Calculation of light scattering from a spherical particle on a surface by the multipole expansion method, J. Opt. Soc. Am. A 13 (1996) 326–336.

[5] Y. Eremin, N. Orlov, Simulation of light scattering from a particle upon a wafer surface, Appl. Opt. 35 (1996) 6599–6604.
[6] Y. Eremin, J.C. Stover, N.V. Orlov, Modeling scatter from silicon wafers features based on discrete sources method, Opt. Eng. 38 (1999) 1296–1304.
[7] T. Wriedt, A. Doicu, Light scattering from a particle on or a near a surface, Opt. Commun. 152 (1998) 376–384.
[8] A. Doicu, Y. Eremin, T. Wriedt, Convergence of the T-matrix method for light scattering from a particle on or near a surface, Opt. Commun. 159 (1999) 266–277.
[9] Yu.A. Eremin, A.G. Sveshnikov, The discrete sources method for investigating three-dimensional electromagnetic scattering problems, Electromagnetics 13 (1993) 1–22.
[10] P.C. Waterman, New formulation of acoustic scattering, J. Acoust. Soc. Am. 45 (1969) 1417–1429.
[11] P.W. Barber, S.C. Hill, Light Scattering by Particles: Computational Methods, World Scientific, Singapore, 1990.